The Astronomical Journal, 131:1461–1470, 2006 March

THE PROPER MOTION OF THE LARGE MAGELLANIC CLOUD: A REANALYSIS

Mario H. Pedreros[1]
Departamento de Física, Facultad de Ciencias, Universidad de Tarapacá, Casilla 7-D, Arica, Chile; mpedrero@uta.cl

and

Edgardo Costa[1] and René A. Méndez[1]
Departamento de Astronomía, Universidad de Chile, Casilla 36-D, Santiago, Chile; costa@das.uchile.cl, rmendez@das.uchile.cl
Received 2005 July 21; accepted 2005 November 17

ABSTRACT

We have determined the proper motion (PM) of the Large Magellanic Cloud (LMC) relative to four background quasi-stellar objects, combining data from two previous studies made by our group and new observations carried out in three epochs not included in the original investigations. The new observations provided a significant increase in the time base and the number of frames, relative to what was available in our previous studies. We have derived a total LMC PM of $\mu = (+2.0 \pm 0.1)$ mas yr^{-1}, with a position angle of $\theta = 62\overset{\circ}{.}4 \pm 3\overset{\circ}{.}1$. Our new values agree well with most results obtained by other authors, and we believe we have clarified the large discrepancy between previous results from our group. Using published values of the radial velocity for the center of the LMC, in combination with the transverse velocity vector derived from our measured PM, we have calculated the absolute space velocity of the LMC. This value, along with some assumptions regarding the mass distribution of the Galaxy, has in turn been used to calculate the mass of the Milky Way. Our measured PM also indicates that the LMC is not a member of a proposed stream of galaxies with similar orbits around our Galaxy.

Key words: astrometry — Magellanic Clouds — quasars: general

1. INTRODUCTION

The present study is a follow-up of the works by Anguita et al. (2000, hereafter ALP00) and Pedreros et al. (2002, hereafter PAM02) in which the proper motion (PM) of the Large Magellanic Cloud (LMC) was determined using the "quasar method." This method, fully described in ALP00 and PAM02, consists of using quasi-stellar objects (QSOs) in the background field of the LMC as fiducial reference points to determine its PM. In this method, the position of the background QSOs is measured at different epochs with respect to bona fide field stars of the LMC that define a local reference system (LRS). Because a QSO can be considered a fiducial reference point, any motion detected will be a reflection of the motion of the LRS of LMC stars.

As shown in Table 1, there is a rather large discrepancy, particularly in declination, between the PM of the LMC derived by ALP00 and that derived by PAM02, with ALP00 − PAM02 differences of −0.3 mas yr^{-1} (1.5 σ) in right ascension and 2.5 mas yr^{-1} (12.5 σ) in declination. This difference prompted us to add new epochs to our database (using the same equipment and setup used by ALP00 and PAM02) and to make a full reanalysis of the entire data set.

Here we report the results obtained, combining data from previous studies by our group with new observations carried out in three additional epochs (not included in the original investigation), for the LMC quasar fields Q0459−6427, Q0557−6713, Q0558−6707, and Q0615−6615 (in the same nomenclature used by ALP00 and PAM02). The original study of field Q0459−6427 was reported in PAM02 and those of Q0557−6713, Q0558−6707, and Q0615−6615 in ALP00. As can be seen in Table 2, which summarizes the total observational material used in the present paper, our new data provide a significant increase in time base and the number of frames, relative to what was available in ALP00 and PAM02. The increase in time base for the fields Q0459−6427, Q0557−6713, Q0558−6707, and Q0615−6615 was 19%, 65%, 126%, and 65%, respectively. The corresponding increase in data points was 7%, 18%, 59%, and 56%, respectively.

2. OBSERVATIONS AND REDUCTIONS

The new observations were carried out with a 24 μm pixels Tektronix 1024 × 1024 CCD detector attached to the Cassegrain focus of the Cerro Tololo Inter-American Observatory 1.5 m telescope in its f/13.5 configuration (scale: $0\overset{''}{.}24$ pixel^{-1}). Only astrometric observations were secured. Because we adopted for each QSO field the same LRS used by ALP00 or PAM02, there was no need for additional photometric observations. Finding charts for the reference stars and the background QSO in each field can be found in ALP00 or PAM02. As in our previous studies, the astrometric observations were made using a Kron-Cousins *R*-band filter, in order to minimize differential color refraction effects.

The method used for the determination of the LMC's PM is the same as that explained in ALP00 and PAM02. Only data not included in those two previous studies went through the full reduction procedure. For data already included in those studies, we used the available raw coordinates for the centroids of the reference stars and background QSOs. Both the existing and the newly determined raw coordinates were treated by means of the same custom programs used in PAM02.

In brief, the (x, y)-coordinates of the QSO and the LMC field reference stars in each image were determined using the DAOPHOT package (Stetson 1987) and then corrected for differential color refraction and transformed to barycentric

[1] Visiting Astronomer, Cerro Tololo Inter-American Observatory, National Optical Astronomy Observatory, operated by the Association of Universities for Research in Astronomy, Inc., under cooperative agreement with the National Science Foundation.

TABLE 1
PREVIOUS DETERMINATIONS OF THE LMC PROPER MOTION USING THE QUASAR METHOD

Source	$\mu_\alpha \cos\delta$ (mas yr^{-1})	μ_δ (mas yr^{-1})	Weighted Mean from
ALP00 (LMC center).....	$+1.7 \pm 0.2$	$+2.9 \pm 0.2$	Three fields
PAM02 (LMC center).....	$+2.0 \pm 0.2$	$+0.4 \pm 0.2$	One field

coordinates. Then, by averaging the barycentric coordinates of the best set of consecutive images taken of each QSO field throughout our program, a standard reference frame (SRF) was defined for every field. All images, taken at different epochs, of each field were then referred to its corresponding SRF. This was done through multiple regression analysis by fitting both sets of coordinates to quadratic equations of the form $X = a_0 + a_1x + a_2y + a_3x^2$ and $Y = b_0 + b_1x + b_2y + b_3x^2$, where (X, Y) are the coordinates on the SRF system and (x, y) are the observed barycentric coordinates. It was found that the above transformation equations yielded the best results for the registration in the SRF, showing no remaining systematic trends in the data.

3. RESULTS

Tables 3–6 list the residual PM (relative to the barycenter of the field's SRF) and photometry (from ALP00 or PAM02 and included here for completeness) of the stars defining the LRS in each of our four QSO fields. Star IDs are the same as those in PAM02 and ALP00 for the corresponding fields. The PM uncertainties correspond to the error in the determination of the slope of the best-fit line. Inspection of these tables shows that the PM uncertainty of most of the reference stars is comparable to or larger than their derived PM value, implying that these PMs do not represent internal motions in the LMC.

In Figure 1 we present the PM maps for the reference stars listed in Tables 3–6. The dispersion around the mean turned out to be ±0.34, ±0.79, ±0.54, and ±0.41 mas yr^{-1} in right ascension and ±0.52, ±0.71, ±0.58, and ±0.62 mas yr^{-1} in declination for Q0459−6427, Q0557−6713, Q0558−6707, and Q0615−6615, respectively. Based on the above argument, the scatter seen in the plots probably stems entirely from the random errors in the measurements and does not represent the actual velocity dispersion in the LMC.

In Figure 2 we present position versus epoch diagrams for the QSO fields in right ascension ($\Delta\alpha \cos\delta$) and declination ($\Delta\delta$), where $\Delta\alpha \cos\delta$ and $\Delta\delta$ represent the positions of the QSOs on different CCD frames, relative to the barycenter of the SRF. These diagrams were constructed using individual position data for the QSO in each CCD image as a function of epoch. In Table 7 we give, for each epoch, the mean barycentric positions of the QSOs along with their mean errors, the number of points used to calculate the mean for each coordinate, and the CCD detectors used. Symbol sizes in Figure 2 are proportional to the number of times the measurements yielded the same coordinate value for a particular epoch. The best-fit straight lines resulting from simple linear regression analysis on the data points are also shown. The negative values of the line slopes correspond to the measured PM of the barycenter of the LRS in each QSO field, relative to the SRF.

Table 8 summarizes our results for the measured PM of the LMC. Column (1) gives the quasar identification, columns (2) and (3) give the right ascension and declination components of the LMC's PM (together with their standard deviations), respectively, and columns (4)–(6) give the number of frames, the number of epochs, and the observation period, respectively. It should be noted that the rather small quoted errors for the PM come out directly from what the least-squares fit yields as the uncertainty in the determination of the slope of the best-fit line.

4. COMPARISON TO OTHER PROPER-MOTION WORK

Table 9 lists the results of all available measurements of the LMC's PM having uncertainties smaller than 1 mas yr^{-1} in both components, as well as the reference system used in each case. With the exception of those cases noted "field" in the first column, all the PMs listed in Table 9 are relative to the LMC's center. To facilitate comparisons, we present our current results in both ways. As explained in § 5, our PM values relative to the LMC's center were obtained by correcting the field PM for the rotation of the plane of the LMC.

Our results are in reasonable agreement with most of the available data. They agree particularly well with those of Kroupa et al. (1994), who used the Positions and Proper Motions Star Catalog (PPM; Röser & Bastian 1993) as a reference system, as well as with the *Hubble Space Telescope* (*HST*) results of Kallivayalil et al. (2006), who used QSOs as a reference system. On the other hand, there still is a significant discrepancy with ALP00's result in declination. We further discuss this issue in § 6.

In Table 9 we have not included a recent determination of the LMC's PM by Momany & Zaggia (2005) using the USNO CCD Astrograph Catalog (UCAC2; Zacharias et al. 2004), because, as confirmed by the errors declared by the authors themselves (∼3 mas in both coordinates), the internal accuracy of their methodology is not comparable with ours. Numerous tests carried out by our group favor the use of fiducial reference points in combination with an LRS defined by relatively few, well-studied (bona fide members, free of contamination from neighboring stars, good signal-to-noise ratio, etc.) LMC stars to determine a PM of this nature. Interestingly, their result, $(\mu_\alpha \cos\delta,\ \mu_\delta) \sim (+0.84,\ +4.32)$ mas yr^{-1}, is in reasonable agreement with that of ALP00.

Combining the components given in the last entry of Table 9, we derive a total LMC PM of $\mu = (+2.0 \pm 0.1)$ mas yr^{-1}, with a position angle of $\theta = 62\overset{\circ}{.}4 \pm 3\overset{\circ}{.}1$, measured eastward from the

TABLE 2
OBSERVATIONAL MATERIAL FOR THE LMC QSO FIELDS

Field	Source	Epochs	Number of Frames (Old Data)	Epoch Range	Epochs	Number of Frames (New Data)	Epoch Range
Q0459−6427.....	PAM02	8	44	1989.91–2000.01	1	3	2001.96
Q0557−6713.....	ALP00	11	61	1989.02–1996.86	2	11	1998.88–2001.96
Q0558−6707.....	ALP00	6	32	1992.81–1996.86	3	19	1998.88–2001.96
Q0615−6615.....	ALP00	8	32	1989.90–1997.19	3	18	1998.88–2001.96

TABLE 3

LOCAL REFERENCE SYSTEM FOR THE Q0459−6427 FIELD

Star ID[a]	$\mu_\alpha \cos\delta$ (mas yr^{-1})	σ (mas yr^{-1})	μ_δ (mas yr^{-1})	σ (mas yr^{-1})	V (mag)	$B-V$ (mag)	$V-R$ (mag)
1	0.0	0.3	+0.9	0.2	18.71	0.95	0.52
2	−0.7	0.3	−0.3	0.4	19.01	0.67	0.38
3	+0.6	0.2	−0.4	0.2	19.02	0.86	0.47
4	0.0	0.3	0.0	0.3	18.88	0.96	0.52
5	0.0	0.3	+0.6	0.3	18.71	0.98	0.54
6	−0.1	0.2	−0.4	0.2	18.22	1.03	0.58
7	+0.1	0.2	+0.1	0.2	18.08	1.03	0.57
8	0.0	0.5	−0.1	0.4	17.98	0.89	0.52
9	+0.1	0.3	−0.6	0.4	19.18	0.84	0.43
10	+0.3	0.1	0.0	0.2	17.94	1.15	0.63
11	0.0	0.3	+0.4	0.3	18.64	0.91	0.50
12	−0.3	0.3	−1.2	0.3	19.03	0.88	0.48
13	+0.4	0.3	+0.6	0.3	18.98	0.86	0.48
14	−0.7	0.3	+0.1	0.3	18.66	0.23	0.03
15	+0.2	0.1	−0.1	0.2	17.70	1.08	0.59
16	+0.4	0.2	+0.3	0.2	16.70	1.43	0.82
17	−0.3	0.2	+0.3	0.2	19.17	0.95	0.51

[a] Star IDs are the same as those in PAM02.

TABLE 4

LOCAL REFERENCE SYSTEM FOR THE Q0557−6713 FIELD

Star ID[a]	$\mu_\alpha \cos\delta$ (mas yr^{-1})	σ (mas yr^{-1})	μ_δ (mas yr^{-1})	σ (mas yr^{-1})	V (mag)	$B-V$ (mag)	$V-R$ (mag)
1	−0.1	0.1	−0.1	0.2	17.07	−0.07	−0.04
2	+0.5	0.2	0.0	0.1	17.75	1.14	0.56
3	−0.1	0.2	+0.7	0.2	18.35	0.84	0.45
4	+0.2	0.3	+2.0	0.3	18.64	0.68	0.38
5	−0.2	0.4	−0.9	0.2	16.93	1.13	0.55
6	+0.6	0.2	−0.5	0.2	17.72	1.22	0.62
7	−0.9	0.3	−0.3	0.3	18.73	1.09	0.48
8	−1.2	0.2	−0.3	0.2	17.29	0.83	0.46
9	+1.5	0.3	+0.4	0.6	18.52	1.00	0.52
10	−1.7	0.6	−1.2	0.3	18.28	0.00	−0.05
11	+0.4	0.2	−0.4	0.2	17.34	1.17	0.56
12	−0.6	0.3	+0.3	0.2	18.66	1.00	0.48
13	−0.4	0.2	−0.4	0.2	18.23	0.75	0.37
14	+1.7	0.3	+0.8	0.3	18.13	0.82	0.42
15	+0.8	0.3	−0.4	0.2	18.48	0.80	0.43
16	+0.4	0.2	−0.1	0.2	18.26	1.09	0.53
17	+0.1	0.2	−0.6	0.2	17.78	0.95	0.51
18	+0.5	0.4	−0.4	0.3	17.57	−0.12	−0.06
19	+0.1	0.1	−0.3	0.2	17.21	1.19	0.63
20	−0.9	0.3	+0.1	0.3	18.69	0.99	0.50
21	−0.3	0.1	+0.4	0.2	17.30	0.77	0.38
22	0.0	0.3	+1.2	0.3	18.05	−0.08	−0.08
23	0.0	0.1	+0.4	0.2	16.23	−0.17	−0.09

[a] Star IDs are the same as those in ALP00.

TABLE 5

LOCAL REFERENCE SYSTEM FOR THE Q0558−6707 FIELD

Star ID[a]	$\mu_\alpha \cos\delta$ (mas yr^{-1})	σ (mas yr^{-1})	μ_δ (mas yr^{-1})	σ (mas yr^{-1})	V (mag)	$B-V$ (mag)	$V-R$ (mag)
1	+0.8	0.5	−0.8	0.7	18.94	0.84	0.44
2	−0.7	0.4	−1.1	0.4	16.44	1.78	0.91
3	+0.2	0.3	−1.2	0.4	17.88	0.90	0.46
4	+0.8	0.5	−0.4	0.6	18.94	0.85	0.46
5	−0.9	0.3	−1.0	0.7	19.01	0.90	0.44
6	−0.7	0.2	+0.6	0.2	18.30	0.88	0.49
7	+0.5	0.2	+0.1	0.3	17.78	1.18	0.62
8	+1.1	0.4	+0.8	0.4	18.36	...	−0.11
9	+0.2	0.2	−0.4	0.2	17.39	1.34	0.70
10	+0.5	0.2	+0.1	0.3	18.43	0.86	0.46
11	−0.8	0.2	+0.8	0.2	17.79	1.13	0.59
12	0.0	0.2	0.0	0.3	18.59	0.88	0.45
13	−0.2	0.3	−0.4	0.4	18.34	−0.02	0.00
14	0.0	0.4	+0.7	0.4	18.20	0.01	−0.01
15	−0.6	0.2	+0.6	0.2	17.44	1.26	0.66
16	−0.7	0.4	+0.7	0.5	19.00	0.91	0.49
17	−0.7	0.3	+1.1	0.3	18.48	0.69	0.40
18	−0.1	0.5	+0.6	0.6	18.98	0.90	0.48
19	+0.2	0.3	+0.7	0.4	18.32	−0.13	−0.02
20	−0.4	0.4	+0.8	0.5	19.00	0.87	0.49
21	+0.4	0.3	+0.4	0.5	18.84	0.91	0.48
22	−0.3	0.4	+0.3	0.4	18.83	0.91	0.48
23	−0.4	0.4	−0.2	0.2	16.29	0.02	0.17
24	0.0	0.2	−0.2	0.2	17.56	1.27	0.67
25	+0.2	0.2	−0.1	0.3	17.69	1.15	0.60
26	+0.2	0.2	+0.1	0.4	18.72	1.20	0.57
27	−0.1	0.2	−0.3	0.3	18.66	1.00	0.54
28	−0.6	0.2	+0.3	0.2	17.31	1.25	0.64
29	+0.6	0.4	−0.2	0.4	18.92	0.89	0.47
30	−0.4	0.3	−0.1	0.3	18.18	1.25	0.59
31	+0.8	0.3	−0.3	0.3	18.55	1.01	0.54
32	+0.2	0.3	−0.4	0.3	18.07	1.12	0.61
33	+0.6	0.2	+0.2	0.2	17.12	1.46	0.76
34	+0.9	0.8	+0.3	0.8	18.68	0.84	0.48
35	+0.2	0.2	−0.6	0.2	17.42	0.90	0.47
36	+0.1	0.3	−0.7	0.4	18.75	0.83	0.45
37	−0.4	0.3	−0.8	0.2	18.65	1.27	0.56
38	0.0	0.2	−0.5	0.2	17.89	1.18	0.60
39	+0.1	0.4	−0.1	0.4	19.12	0.92	0.50
40	−0.7	0.4	−0.1	0.4	19.05	0.88	0.50
41	+0.3	0.2	−0.2	0.4	18.35	0.01	0.02
42	−0.2	0.2	−0.9	0.5	18.58	0.89	0.50
43	+0.1	0.2	0.0	0.2	17.45	1.32	0.68
44	+0.3	0.5	0.0	0.6	19.01	0.85	0.49
45	0.0	0.3	+1.3	0.3	18.46	0.66	0.43
46	−0.8	0.3	+0.5	0.4	19.05	0.86	0.52
47	−0.4	0.4	+0.7	0.6	19.04	1.01	0.54
48	+0.5	0.2	+0.6	0.3	16.81	0.08	0.06
49	+1.2	0.4	0.0	0.3	19.04	0.83	0.49
50	−1.0	0.3	−0.5	0.3	17.76	1.07	0.57
51	−0.2	0.3	−0.8	0.3	18.16	0.83	0.48
52	−0.3	0.4	0.0	0.5	18.93	0.89	0.46

[a] Star IDs are the same as those in ALP00.

TABLE 6

LOCAL REFERENCE SYSTEM FOR THE Q0615−6615 FIELD

Star ID[a]	$\mu_\alpha \cos\delta$ (mas yr^{-1})	σ (mas yr^{-1})	μ_δ (mas yr^{-1})	σ (mas yr^{-1})	V (mag)	$B-V$ (mag)	$V-R$ (mag)
1.....	0.0	0.2	+0.1	0.4	18.95	0.87	0.53
2.....	0.0	0.2	+0.7	0.3	18.29	0.83	0.47
3.....	−0.1	0.2	−0.4	0.3	17.46	0.75	0.43
4.....	0.0	0.3	−1.0	0.4	19.14	0.61	0.41
5.....	−0.2	0.2	+0.3	0.2	18.23	0.76	0.45
6.....	+0.4	0.3	+0.9	0.3	19.00	0.98	0.56
7.....	−0.6	0.2	−0.4	0.2	19.07	0.65	0.42
8.....	+0.7	0.2	+0.1	0.2	18.37	0.89	0.53
9.....	−0.2	0.4	+0.7	0.5	18.98	0.84	0.49
10.....	−0.2	0.3	−0.9	0.4	18.85	0.85	0.48
11.....	0.0	0.3	−0.3	0.4	18.97	...	0.73
12.....	0.0	0.2	−0.7	0.2	18.25	1.07	0.53
13.....	−0.1	0.2	0.0	0.3	17.59	1.04	0.65
14.....	+0.7	0.2	+0.8	0.2	18.33	1.00	0.57
15.....	+0.4	0.4	−0.6	0.5	19.36	0.90	0.50
16.....	−0.9	0.4	+0.6	0.5	19.29	0.81	0.47

[a] Star IDs are the same as those in ALP00.

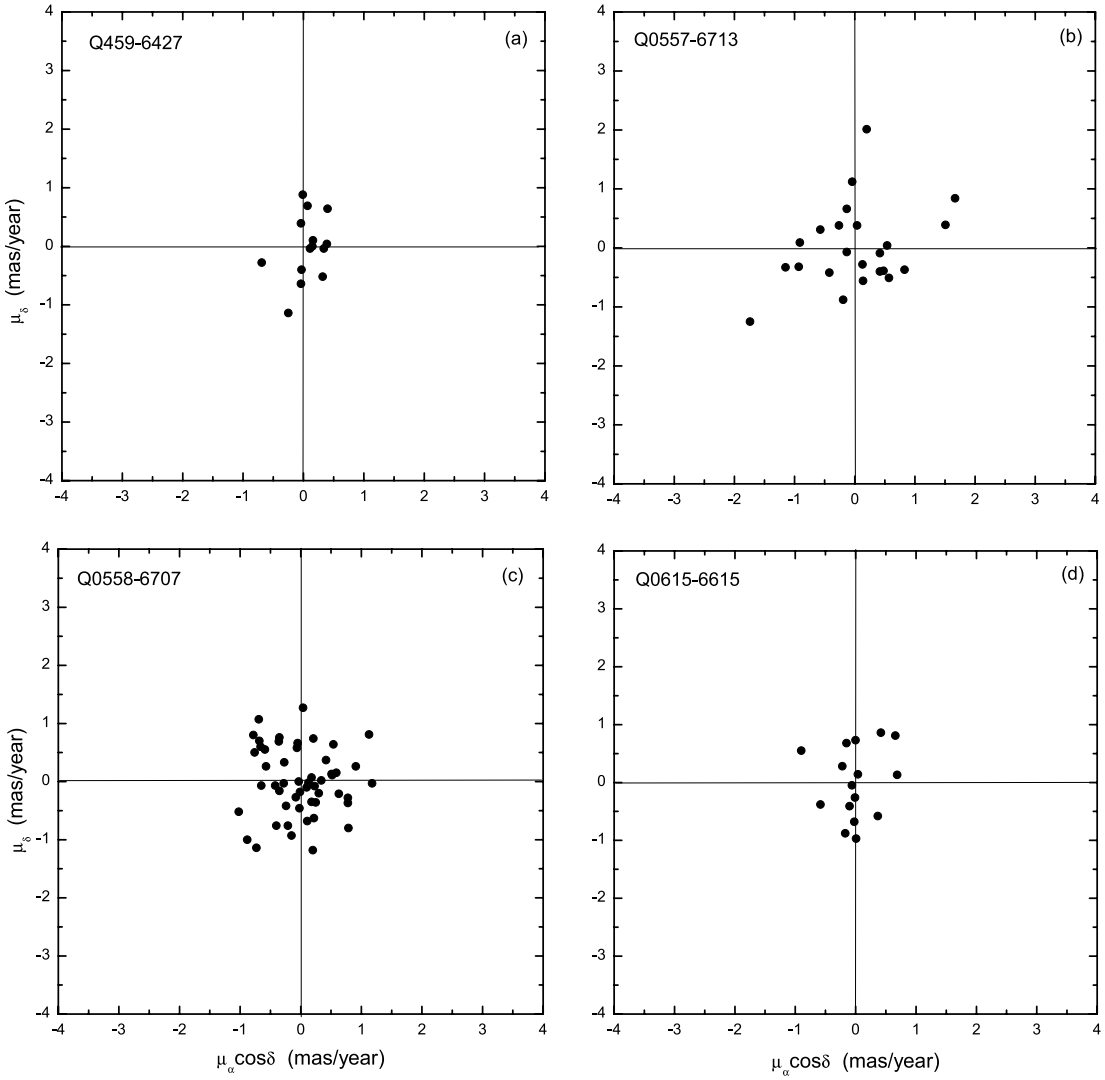

FIG. 1.—Residual PM maps for the reference stars listed in Tables 3–6. The dispersion around the mean is ±0.34, ±0.79, ±0.54, and ±0.41 mas yr^{-1} in right ascension and ±0.52, ±0.71, ±0.58, and ±0.62 mas yr^{-1} in declination for Q0459−6427, Q0557−6713, Q0558−6707, and Q0615−6615, respectively.

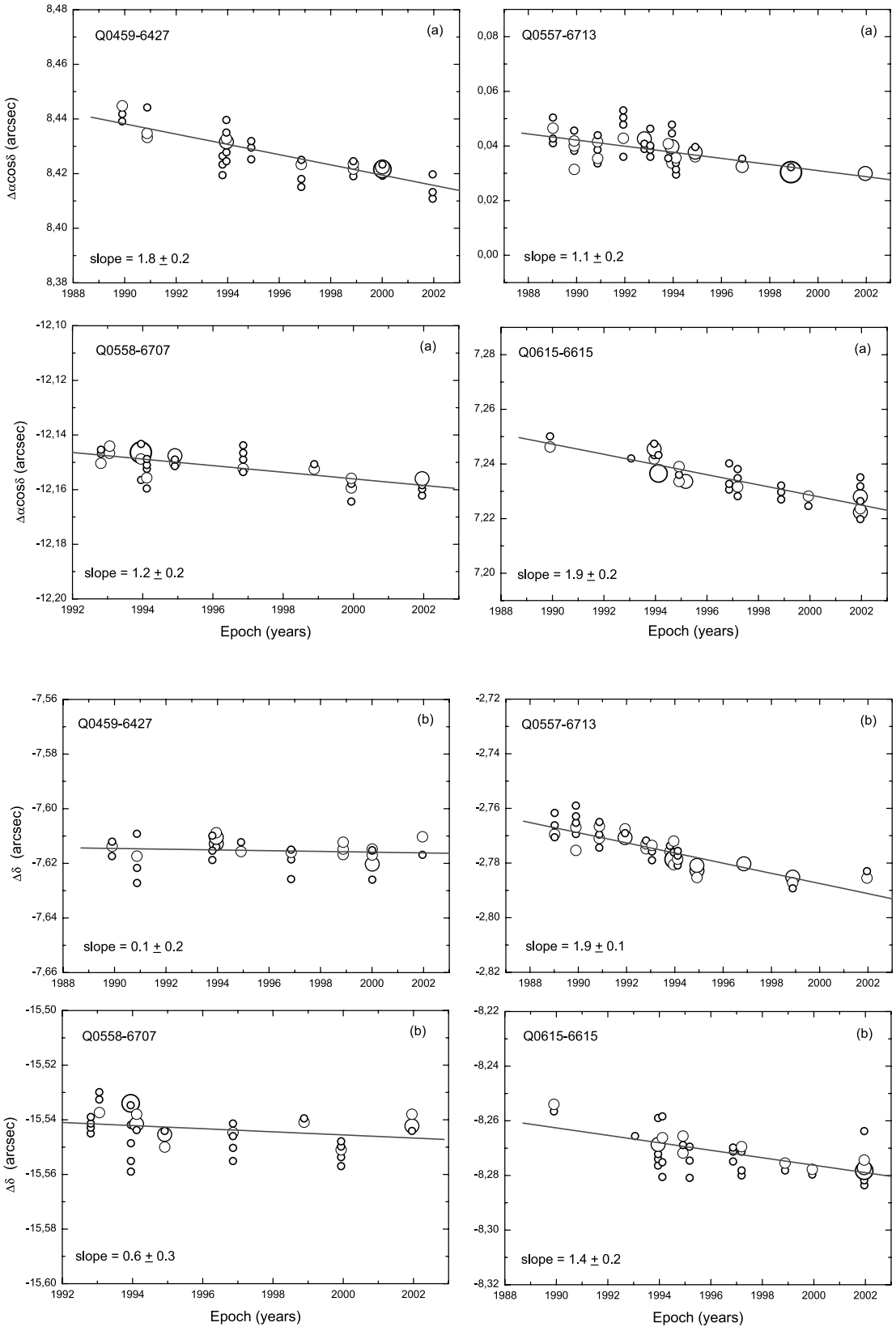

FIG. 2.—(*a*) Relative positions in right ascension ($\Delta\alpha \cos\delta$) vs. epoch of observation for the studied fields. The values of $\Delta\alpha \cos\delta$ represent the individual positions of the QSO on different CCD frames relative to the barycenter of the SRF. Symbol sizes are proportional to the number of times the measurements yielded the same coordinate value for a particular epoch (extra-small, small, medium, large, and extra-large sizes indicate one to five measurements per epoch, respectively). The best-fit straight lines from linear regression analyses on the data are also shown. (*b*) Same as (*a*), but for declination ($\Delta\delta$).

TABLE 7

MEAN BARYCENTRIC POSITIONS OF QUASARS IN THE LMC

Epoch	$\Delta\alpha \cos\delta$ (arcsec)	σ (mas)	$\Delta\delta$ (arcsec)	σ (mas)	N	CCD Chip
			Q0459−6427			
1989.907	8.443	1.4	−7.614	1.1	4	RCA No. 5
1990.872	8.434	0.3	−7.615	2.7	3	Tek No. 4
1990.878	8.438	5.8	−7.624	2.8	2	RCA No. 5
1993.800	8.423	2.0	−7.615	2.6	3	Tek 1024 No. 1
1993.953	8.432	1.4	−7.611	0.7	9	Tek 1024 No. 2
1994.916	8.429	2.0	−7.615	1.1	3	Tek 1024 No. 2
1996.860	8.421	1.9	−7.618	2.0	5	Tek 2048 No. 4
1998.881	8.422	0.8	−7.615	0.8	6	Tek 1024 No. 2
2000.010	8.422	0.4	−7.618	1.2	9	Tek 1024 No. 2
2001.961	8.416	2.1	−7.612	2.9	3	Tek 1024 No. 2
			Q0557−6713			
1989.024	0.045	1.6	−2.768	1.6	5	RCA No. 5
1989.905	0.039	1.8	−2.768	1.9	8	RCA No. 5
1990.872	0.037	1.6	−2.772	1.0	4	Tek No. 4
1990.878	0.040	2.7	−2.766	0.5	3	RCA No. 5
1991.938	0.046	2.5	−2.769	0.7	6	Tek 1024 No. 1
1992.812	0.042	0.7	−2.774	0.6	5	Tek 2048 No. 1
1993.055	0.040	2.2	−2.776	1.3	4	Tek 1024 No. 1
1993.800	0.039	1.8	−2.775	0.7	3	Tek 1024 No. 1
1993.953	0.039	1.5	−2.777	1.1	9	Tek 1024 No. 2
1994.119	0.033	1.2	−2.778	0.9	5	Tek 1024 No. 2
1994.918	0.036	0.8	−2.783	0.7	8	Tek 1024 No. 2
1996.862	0.033	0.9	−2.780	0.3	3	Tek 2048 No. 4
1998.883	0.031	0.3	−2.786	0.7	6	Tek 1024 No. 2
2001.961	0.030	0.3	−2.785	0.9	3	Tek 1024 No. 2
			Q0558−6707			
1992.813	−12.148	1.3	−15.542	1.3	4	Tek 2048 No. 1
1993.058	−12.145	0.8	−15.534	1.8	4	Tek 1024 No. 1
1993.953	−12.148	1.2	−15.542	3.4	9	Tek 1024 No. 2
1994.118	−12.154	1.6	−15.541	1.0	6	Tek 1024 No. 2
1994.918	−12.149	0.6	−15.547	0.9	7	Tek 1024 No. 2
1996.863	−12.150	1.6	−15.547	2.0	6	Tek 2048 No. 4
1998.886	−12.152	0.7	−15.540	0.5	3	Tek 1024 No. 2
1999.942	−12.159	1.3	−15.552	1.3	6	Tek 1024 No. 2
2001.958	−12.158	1.1	−15.541	1.1	6	Tek 1024 No. 2
			Q0615−6615			
1989.908	7.248	1.3	−8.255	0.9	3	RCA No. 5
1993.058	7.242	...	−8.266	...	1	Tek 1024 No. 1
1993.953	7.244	0.8	−8.270	2.1	7	Tek 1024 No. 2
1994.120	7.238	1.3	−8.269	3.9	5	Tek 1024 No. 2
1994.920	7.236	1.2	−8.269	1.4	5	Tek 1024 No. 2
1995.178	7.234	0.2	−8.275	3.3	3	Tek 1024 No. 2
1996.864	7.234	2.9	−8.272	1.5	3	Tek 2048 No. 4
1997.194	7.233	1.7	−8.274	2.2	5	Tek 1024 No. 2
1998.886	7.230	1.5	−8.276	1.0	3	Tek 1024 No. 2
1999.942	7.227	1.2	−8.278	0.8	3	Tek 1024 No. 2
2001.960	7.226	1.3	−8.277	1.4	12	Tek 1024 No. 2

TABLE 8

PROPER MOTION OF THE LMC (AS MEASURED)

Field ID (1)	$\mu_\alpha \cos\delta$ (mas yr^{-1}) (2)	μ_δ (mas yr^{-1}) (3)	Number of Frames (4)	Epochs (5)	Epoch Range (6)
Q0459−6427	1.8 ± 0.2	0.1 ± 0.2	47	9	1989.91–2001.96
Q0557−6713	1.1 ± 0.2	1.9 ± 0.1	72	13	1989.02–2001.96
Q0558−6707	1.2 ± 0.2	0.6 ± 0.3	51	9	1992.81–2001.96
Q0615−6615	1.9 ± 0.2	1.4 ± 0.2	50	11	1989.90–2001.96

TABLE 9
HIGH-PRECISION DETERMINATIONS OF THE PROPER MOTION OF THE LMC

Source	$\mu_\alpha \cos\delta$ (mas yr^{-1})	μ_δ (mas yr^{-1})	Proper-Motion System
Kroupa et al. 1994 (field)	+1.3 ± 0.6	+1.1 ± 0.7	PPM
Jones et al. 1994	+1.37 ± 0.28	−0.18 ± 0.27	Galaxies
Kroupa & Bastian 1997 (field)	+1.94 ± 0.29	−0.14 ± 0.36	*Hipparcos*
ALP00	+1.7 ± 0.2	+2.9 ± 0.2	Quasars
PAM02	+2.0 ± 0.2	+0.4 ± 0.2	Quasars
Drake et al. 2001	+1.4 ± 0.4	+0.38 ± 0.25	Quasars
Kallivayalil et al. 2006	+2.03 ± 0.08	+0.44 ± 0.05	Quasars
This work (field)[a]	+1.5 ± 0.1	+1.4 ± 0.1	Quasars
This work[a]	+1.8 ± 0.1	+0.9 ± 0.1	Quasars

[a] Weighted mean of our four QSO fields.

meridian joining the center of the LMC to the north celestial pole. This result is compatible (particularly the PM's absolute value) with theoretical models (Gardiner et al. 1994), which predict a PM for the LMC in the range 1.5–2.0 mas yr^{-1}, with a position angle of $\theta \approx 90^\circ$.

5. SPATIAL VELOCITY OF THE LMC AND MASS OF THE GALAXY

Using the PM of the LMC determined in § 3 and the radial velocity of its center (adopted from the literature), we can calculate the radial and transverse components of the velocity for the LMC as seen from the center of the Galaxy, along with other parameters described below. To do this we basically followed the procedure outlined by Jones et al. (1994). In the calculations, we used as basic LMC parameters those given in Table 8 of ALP00 and assumed a rotational velocity $v_\Phi = 50$ km s^{-1} and a radial velocity $V_r = 250$ km s^{-1} for the LMC.

In order to determine, from our measured PM values, the space velocity components of the LMC and its PM with respect to the Galactic rest frame (GRF), a series of steps were required. These included (1) a correction to our measured PM values to account for the rotation of the plane of the LMC and (2) a transformation of the corrected PM into transverse velocity components with respect to the center of the LMC, the Sun, the LSR, and the center of the Galaxy (both in the equatorial and galactic coordinate systems). These transverse velocities, in combination with the radial velocity of the center of the LMC (adopted from the literature), allowed us to derive the components of the space velocity of the LMC, corrected for the Sun's peculiar motion relative to the LSR and for the velocity of the LSR itself, relative to the center of the Galaxy. The above calculations were made using an ad hoc computer program, developed by one of the authors (M. H. P.), which generates results consistent with those from independent software (S. Piatek 2005; private communication).

The results of the above procedure applied to our four quasar fields are presented in Table 10. In the first and second rows we list the right ascension and declination corrections to our measured PM to account for the rotation of the plane of the LMC, and in the third and fourth rows we list the corresponding corrected PM values, in equatorial coordinates, as viewed by an observer located at the center of the LMC. In the fifth through eighth rows we give calculated PM values relative to the GRF both in equatorial and galactic coordinates. These values correspond to the LMC's PM as seen by an observer located at the Sun, with the contributions to the PM from the peculiar solar motion and the LSR's motion removed. In the ninth, tenth, and eleventh rows we give the Π, Θ, and Z components, respectively, of the space velocity in a rectangular Cartesian coordinate system centered on the LMC (as defined by Schweitzer et al. [1995] for the Sculptor dwarf spheroidal galaxy). The Π component is parallel to the projection onto the Galactic plane of the radius vector from the center of the Galaxy to the center of the LMC and is positive when it points radially away from the Galactic center. The Θ component is perpendicular to the Π component, parallel to the Galactic plane, and points in the direction of rotation of the Galactic disk. The Z component points in the direction of the north Galactic pole. These three components are free from the Sun's

TABLE 10
PROPER-MOTION AND SPACE VELOCITY RESULTS FOR THE LMC

Parameter	Q0459−6427	Q0557−6713	Q0558−6707	Q0615−6615
$\Delta\mu_\alpha \cos\delta$, rotation correction (mas yr^{-1})	+0.17	+0.11	+0.11	+0.12
$\Delta\mu_\delta$, rotation correction (mas yr^{-1})	+0.09	−0.18	−0.18	−0.18
$\mu_\alpha^{\rm LMC} \cos\delta$, LMC centered (mas yr^{-1})	1.9 ± 0.2	1.5 ± 0.2	1.4 ± 0.2	2.2 ± 0.2
$\mu_\delta^{\rm LMC}$, LMC centered (mas yr^{-1})	0.5 ± 0.2	1.5 ± 0.1	0.2 ± 0.2	0.7 ± 0.2
$\mu_\alpha^{\rm GRF} \cos\delta$ (mas yr^{-1})	1.4 ± 0.1	1.0 ± 0.1	0.9 ± 0.1	1.7 ± 0.1
$\mu_\delta^{\rm GRF}$ (mas yr^{-1})	0.4 ± 0.2	1.3 ± 0.1	0.1 ± 0.3	0.6 ± 0.2
$\mu_l^{\rm GRF} \cos b$ (mas yr^{-1})	−0.6 ± 0.2	−1.5 ± 0.1	−0.3 ± 0.3	−0.9 ± 0.2
$\mu_b^{\rm GRF}$ (mas yr^{-1})	1.4 ± 0.1	0.7 ± 0.1	0.8 ± 0.1	1.5 ± 0.1
Π, velocity component (km s^{-1})	252 ± 25	215 ± 23	171 ± 28	292 ± 23
Θ, velocity component (km s^{-1})	93 ± 41	319 ± 31	27 ± 63	160 ± 45
Z, velocity component (km s^{-1})	234 ± 25	109 ± 24	135 ± 26	274 ± 22
$V_{{\rm gc},r}$, radial velocity (km s^{-1})	80 ± 23	118 ± 22	68 ± 24	92 ± 20
$V_{{\rm gc},t}$, transverse velocity (km s^{-1})	347 ± 27	382 ± 30	209 ± 27	421 ± 27

TABLE 11
MASS OF THE GALAXY FOR THREE LMC ROTATIONAL VELOCITIES

Parameter	Q0459−6427	Q0557−6713	Q0558−6707	Q0615−6615
	$v_\Phi = 50$ km s^{-1}			
$V_{gc,r}$, radial velocity (km s^{-1})	80 ± 23	118 ± 22	68 ± 24	92 ± 20
$V_{gc,t}$, transverse velocity (km s^{-1})	347 ± 27	382 ± 30	209 ± 27	421 ± 27
M_G, mass of the Galaxy × 10^{11} $M_\odot$	(8.2 ± 1.3)	(9.9 ± 1.6)	(3.0 ± 0.8)	(12 ± 2)
	$v_\Phi = 0$ km s^{-1}			
$V_{gc,r}$, radial velocity (km s^{-1})	75 ± 23	126 ± 22	75 ± 24	99 ± 20
$V_{gc,t}$, transverse velocity (km s^{-1})	305 ± 26	408 ± 30	198 ± 33	420 ± 30
M_G, mass of the Galaxy × 10^{11} $M_\odot$	(6.3 ± 1.1)	(11 ± 2)	(2.7 ± 0.9)	(12 ± 2)
	$v_\Phi = 90$ km s^{-1}			
$V_{gc,r}$, radial velocity (km s^{-1})	83 ± 23	112 ± 22	62 ± 24	86 ± 20
$V_{gc,t}$, transverse velocity (km s^{-1})	381 ± 27	364 ± 29	225 ± 26	425 ± 25
M_G, mass of the Galaxy × 10^{11} $M_\odot$	(9.9 ± 1.4)	(9.0 ± 1.5)	(3.4 ± 0.8)	(12 ± 2)

peculiar motion and LSR motion. In the last two rows we give the LMC's radial and transverse space velocities, as seen by a hypothetical observer located at the center of the Galaxy and at rest with respect to the Galactic center.

All of the above calculations were carried out assuming a distance of 50.1 kpc from the LMC to the Sun, a distance of 8.5 kpc from the Sun to the Galactic center, a 220 km s^{-1} circular velocity of the LSR, and a peculiar velocity of the Sun relative to the LSR of $(u_\odot,\ v_\odot,\ w_\odot) = (-10,\ 5.25,\ 7.17)$ km s^{-1} (Dehnen & Binney 1998). These components are positive if $u_\odot$ points radially away from the Galactic center, $v_\odot$ points in the direction of Galactic rotation, and $w_\odot$ is directed toward the north Galactic pole. Although the matter was not addressed here, the values presented in Table 10 can be used to determine the orbit of the LMC and, therefore, to study possible past and future interactions of the LMC with other Local Group galaxies.

If we assume that the LMC is gravitationally bound to, and in an elliptical orbit around, the Galaxy, and that the mass of the Galaxy is contained within 50 kpc of the Galactic center, we can make an estimate of the lower limit of its mass through the expression

$$M_G = (r_{LMC}/2G)[V_{gc,r}^2 + V_{gc,t}^2(1 - r_{LMC}^2/r_a^2)]/(1 - r_{LMC}/r_a),$$

where r_a is the LMC's apogalacticon distance and r_{LMC} is its present distance.

For $r_a = 300$ kpc (Lin et al. 1995) we obtain M_G values of (8.2 ± 1.3), (9.9 ± 1.6), (3.0 ± 0.8), and (12 ± 2) × 10^{11} $M_\odot$ for the fields Q0459−6427, Q0557−6713, Q0558−6707, and Q0615−6615, respectively. The above values result in a weighted average of $\langle M_G \rangle = (5.9 \pm 0.6) \times 10^{11}\ M_\odot$ for the estimated mass of our Galaxy enclosed within 50 kpc.

To evaluate the effect of the rotational velocity of the LMC on the determination of the mass of our Galaxy, we also carried out calculations using the extreme values $v_\Phi = 0$ km s^{-1} (zero rotation) and $v_\Phi = 90$ km s^{-1}. The weighted mass averages for 0 and 90 km s^{-1} were (5.6 ± 0.6) × 10^{11} and (6.3 ± 0.6) × 10^{11} $M_\odot$, respectively. Our results are summarized in Table 11.

It should be noted that, although slightly larger, all our values for M_G are compatible with the recent theoretical $5.5 \times 10^{11}\ M_\odot$ upper mass limit of the Galaxy given by Sakamoto et al. (2003). They are also compatible with the assumption that the LMC is bound to the Galaxy.

6. DISCUSSION

6.1. *The ALP00-PAM02 Discrepancy*

Given the implications of the result obtained by ALP00 for the PM of the LMC, in relation to our understanding of the interactions between the Galaxy and the Magellanic Clouds (see, e.g., Momany & Zaggia 2005), and the reality of streams of galaxies with similar orbits around the Galaxy (see, e.g., Piatek et al. 2005), the main objective of the present work was to clarify the discrepancy between the previous determinations of the PM of the LMC by our group: the "ALP00-PAM02 Discrepancy." In this section we further elaborate on some of the thoughts originally proposed in PAM02 in order to explain the discrepancy of ALP00, originally with PAM02 and now also with the new result presented in this paper.

First, the fact that the observations used here were made with essentially the same equipment and instrumental setup as those by ALP00 precludes any arguments relating the observed discrepancy to the existence of systematic errors in the observational data. Such errors would affect our data in the same way as those of ALP00.

Second (as explained in § 2), in the reduction process of the ALP00 and PAM02 data incorporated in the present work, we adopted the same QSO and reference-star centroid coordinates (x, y) used in those works. Furthermore, the new data included in the present calculations were processed using the same procedure used in ALP00 to obtain the (x, y)-coordinates. Therefore, the centroid coordinates should not be a source of systematic error either.

The subsequent procedures to obtain the PM were also basically the same, the sole exception being the inclusion of a quadratic term in the transformation equations used for the registration (also included in PAM02's equations, but not in ALP00's). Tests carried out using ALP00's data alone showed, however, that the effect of including quadratic terms is marginal (as was suspected) and does not account for the observed discrepancy.

Considering that our current result, which includes reprocessed data from ALP00, agrees quite well with measurements by other groups, we conclude that ALP00's results might be affected by an unidentified systematic error in declination. Since in the present work we used ALP00's unmodified (x, y)-coordinates, we believe that this error could have originated in the processing of the declination PM instead of the coordinates themselves.

It should be pointed out that the UCAC2-based result from Momany & Zaggia (2005), which is consistent with that from ALP00, is currently also considered to be affected by an as-yet unidentified systematic error (Momany & Zaggia 2005; Kallivayalil et al. 2006). Finally, we would like to note that our new result for field Q0459−6427 is consistent with PAM02.

6.2. *Membership of the LMC in a Stream*

Lynden-Bell & Lynden-Bell (1995) have proposed that the LMC, together with the SMC, Draco, and Ursa Minor and possibly Carina and Sculptor, define a stream of galaxies with similar orbits around our Galaxy. Their models predict a PM for each member of the stream that can be compared to their measured PM to evaluate the reality of the stream.

For the LMC they predict PM components of $(\mu_\alpha \cos\delta,\ \mu_\delta) = (+1.5,\ 0)$ mas yr^{-1}, giving a total PM of $\mu = +1.5$ mas yr^{-1}, with a position angle of $\theta = 90^\circ$. A comparison of this prediction with our result [$\mu = (+2.0 \pm 0.1)$ mas yr^{-1}, $\theta = 62\overset{\circ}{.}4 \pm 3\overset{\circ}{.}1$] shows that our measured values of μ and θ are, respectively, 5.1 σ and 8.9 σ away from the predicted values. This result indicates that the LMC does not seem to be a member of the above stream (it is worth mentioning that Piatek et al. [2005], using *HST* data, have concluded that Ursa Minor is not a member of this stream).

M. H. P. is grateful for the support of the Universidad de Tarapacá research fund (project 4722-02). E. C. and R. A. M. acknowledge support by the Fondo Nacional de Investigación Científica y Tecnológica (proyecto 1050718, Fondecyt) and by the Chilean Centro de Astrofísica FONDAP (15010003). It is also a pleasure to thank T. Martínez for helping with data processing. We would like to thank the referee, S. Piatek, for his constructive comments.

REFERENCES

Anguita, C., Loyola, P., & Pedreros, M. H. 2000, AJ, 120, 845 (ALP00)
Dehnen, W., & Binney, J. J. 1998, MNRAS, 298, 387
Drake, A. J., et al. 2001, BAAS, 33, 1379
Gardiner, L. T., Sawa, T., & Fujimoto, M. 1994, MNRAS, 266, 567
Jones, B. F., Klemola, A. R., & Lin, D. N. C. 1994, AJ, 107, 1333
Kallivayalil, N., van der Marel, R. P., Alcock, C., Axelrod, T., Cook, K. H., Drake, A. J., & Geha, M. 2006, ApJ, 638, 772
Kroupa, P., & Bastian, U. 1997, NewA, 2, 77
Kroupa, P., Röser, S., & Bastian, U. 1994, MNRAS, 266, 412
Lin, D. N. C., Klemola, A. R., & Jones, B. F. 1995, ApJ, 439, 652
Lynden-Bell, D., & Lynden-Bell, R. M. 1995, MNRAS, 275, 429
Momany, Y., & Zaggia, S. 2005, A&A, 437, 339
Pedreros, M. H., Anguita, C., & Maza, J. 2002, AJ, 123, 1971 (PAM02)
Piatek, S., Pryor, C., Bristow, P., Olszewski, E. W., Harris, H. C., Mateo, M., Minniti, D., & Tinney, C. G. 2005, AJ, 130, 95
Röser, S., & Bastian, U. 1993, PPM Star Catalogue South: Positions and Proper Motions of 197,179 Stars South of −2.5 Degrees Declination for Equinox and Epoch J2000.0 (Heidelberg: Spektrum Akademischer)
Sakamoto, T., Chiba, M., & Beers, T. C. 2003, A&A, 397, 899
Schweitzer, A. E., Cudworth, K. M., Majewski, S. R., & Suntzeff, N. B. 1995, AJ, 110, 2747
Stetson, P. B. 1987, PASP, 99, 191
Zacharias, N., Urban, S. E., Zacharias, M. I., Wycoff, G. L., Hall, D. M., Monet, D. G., & Rafferty, T. J. 2004, AJ, 127, 3043